Assessing the importance of convective and inductive electric fields in forming the stormtime ring current

M. W. Liemohn and J. U. Kozyra

Space Physics Research Laboratory, University of Michigan
2455 Hayward St., Ann Arbor, MI 48109-2143;
liemohn@umich.edu, jukozyra@umich.edu

Abstract. Data and model results are examined to assess the relative importance of convective and inductive electric fields in allowing plasma sheet access to the inner magnetosphere to form the stormtime ring current. The two main drivers that force ions from the tail into the near-Earth region are the convective drift (driven by dayside reconnection) and the inductive drift (driven by substorms). Observations show that substorms, on average, do not particularly influence the near-Earth plasma sheet ion population at energies below 40 keV. Higher energies, however, are substantially enhanced at substorm expansion phase onset. Simulation results show that the observed ring current energy content (as defined by Dst*) can be almost entirely predicted with the convective inflow of plasma sheet ions at energies below 40 keV. It is concluded that substorms do not directly contribute to an immediate ring current response. The primary influence of substorms on ring current dynamics, therefore, is confined to redistributing the plasma in the magnetotail and enhancing the ionospheric outflow of heavy ions from the nightside auroral zone.

1. Introduction

The growth rate of the ring current is controlled by two main factors: the intensity of the near-Earth plasma sheet particle flux and the intensity of the force pushing these particles into the inner magnetosphere [e.g., *Burton et al*., 1975; *Thomsen et al.*, 1998]. The former can be condensed into a few characteristic numbers describing the plasma, for example density, temperature, anisotropy, and composition. The latter can be divided into several drift components, namely large-scale convection, localized inductive convection during dipolarizations, corotation, and gradient-curvature. Of these four drift terms, the last two are purely azimuthal, so only the first two contribute to the flow of particles into the near-Earth region.

Convective drift is due to the magnetic pressure ibalance between the nightside and dayside magnetosphere, and thus it peaks during periods of strongly southward interplanetary magnetic field (IMF). Inductive drift is caused by the intense electric fields created from magnetotail collapse during substorms. While the former is spread across the entire width of the magnetosphere, the latter is often confined to a narrow channel in local time. Therefore, they are quite different, phenomenologically, and there is some debate about which of these drift processes is more significant. This study addresses the relative importance of convective versus inductive dominance in allowing plasma sheet access to this region.

2. Storms and Substorms

Over forty years ago, the term "substorm" was defined by *Akasofu and Chapman* [1961] as a basic reconfiguration phenomenon of a stressed magnetosphere, choosing the prefix to highlight it as an essential component of magnetic storms. While noting that substorms can occur in isolation, they had not observed a storm with several embedded substorms. Furthermore, the high plasma flow speeds in the magnetotail associated with this transient events were thought to be the primary driver of plasma sheet ions into the ring current around the Earth.

From this initial definition, the opinion that a storm is simply the collection of a series of closely-spaced substorms persisted for many years. The underlying assumption was that, because substorms were the mechanism for creating the ring current, a series of substorms must therefore create a substantial belt of ions in the inner magnetosphere. Eventually, however, *Tsurutani and Gonzalez* [1987] analyzed periods of high-intensity, long-duration, continuous auroral activity (HILD-CAA events), caused by Alfvén wave trains in the solar wind. These disturbed times were distinctly not magnetic storm events, and doubt was cast on the storm-substorm relationship.

In their extensive review of magnetic storms, *Gonzalez et al*. [1994] clarified the issue by concluding that a storm requires not only a series of substorms but also sustained, strong convection. Because of the sinusoidal rotation of the IMF during HILD-CAA events, the convection requirement for storm development is usually not met. *Gonzalez et al*. [1994] redefined the concept of a magnetic storm, but left the details of why convection is a necessary component for later studies.

One such study is *Wolf et al*. [1997], who performed a series of simulations to examine the importance of convection bursts, dayside compressions, and tail field collapses. They found that both the dayside compression and nightside collapse of the magnetic field have very little influence on the development of a stormtime ring current. The largest inner magnetospheric fluxes resulted from a series of strong convection intervals (3 hours on, 3 hours off sequence).

Another study is *Fok et al*. [1999], who showed, also through a series of kinetic simulations, that the dipolarization during a substorm is insufficient to inject many ions from the plasma sheet. The superposition of an intense large-scale electric field during dipolarization brought far more ions into the ring current than either convection or substorms could do alone.

Below, this issue will be addressed by considering recent data analysis studies and examining ring current simulation results to further quantify this relationship. Specifically, the particles that actually create the stormtime ring current are scrutinized to determine the true role of substorms.

3. Observations

Birn et al. [1997a, 1997b] discuss dispersionless substorm injections as measured by several geosynchronously-orbiting spacecraft. Data from two instruments were used, the magnetospheric plasma analyzer (MPA), which measures electrons and ions with energies below 40 keV, and the synchronous orbit particle analyzer (SOPA), which measures electrons and ions above 50 keV. In a superposed epoch analysis of hundreds of events, they determined the typical characteristics of the plasma changes during injections. They show that, on average, there is very little change in the moments of the MPA data (density, temperature, pressure), while the SOPA data show significant increases in these quantities. This trend is clearly seen in the example events they highlighted, with the fluxes from MPA barely reacting at the injection onset while the SOPA channels saw (up to) order of magnitude increases in particle flux. It was concluded that the geosyncrhonous-altitude (6.6 R_E geocentric distance) plasma in the MPA energy range (E<40 keV) is not significantly affected by substorms.

A similar result was found by *Daglis and Axford* [1996] at distances farther from Earth (7-9 R_E) and by *Grande et al.* [1999] at distances closer to Earth 4-7 R_E). Another result from these two studies is that the composition before and after the passage of a substorm injection front are remarkably similar (on average), indicating that the substorm is primarily energizing the preexisting plasma with only a minor composition change resulting from inflow of new plasma in from another location (for instance, from the ionosphere or deep tail).

Evidence for a substorm influence on the E<40 keV energy range in the near-Earth region was found by *Ganushkina et al.* [2000]. They examined nearly 400 nose events, where 20-50 keV ions are seen deep in the inner magnetosphere (creating a "nose" in the energy-time spectrograms). They associated these nose events with enhanced AE, with a high occurrence rate whenever AE went above 150 nT. *Ganushkina et al*. [2001] simulated the timing of the particle injections by superposing a substorm induction electric field model (that of *Li et al.* [1993, 1998]) on a weakly-driven large-scale convection field. They found that the sub-

storm field was necessary to convect the particles to the spacecraft to match the time delay in the observations. It should be noted, however, that the substorm electric field model used for this study has now been revised [*Sarris et al*., 2002], drastically lowering the field intensity near the Earth. Also, the AE level they found is too low of a threshold for defining a substorm. Therefore, it is unclear whether substorms are the true cause of the nose event observations. As a final note, the nose events examined by *Ganushkina et al.* [2000] often had nose flux intensities that were less than the preexisting (often quiet time) ring current (at higher energies), so the impact on the total energy content of the ring current is likely very small.

From these recent observations, it can be concluded that substorms cause a big enhancement of ion fluxes at energies greater than 40 keV in the near-Earth plasma sheet, but there is not much change at lower energies.

4. Simulations

This study continues to examine this issue by considering ring current simulation results. The model is that of *Liemohn et al*. [2001a], a version of the ion transport code originally developed by *Fok et al*. [1993] and *Jordanova et al*. [1996], which solves the gyration and bounce-averaged kinetic equation for the phase space density of hot H^+ and O^+ ions. Using second-order accurate numerical techniques, it calculates density values as a function of time, equatorial radial distance and azimuth, energy, and equatorial pitch angle. It employs a dipole magnetic field and a McIlwain E5D electric field [*McIlwain*, 1986], modified to scale with the cross polar cap potential difference. MPA and SOPA fluxes are used as nightside plasma boundary conditions, with a *Sheldon and Hamilton* [1992] initial condition. Density is lost through a number of processes, including flow through the simulation boundaries, precipitation into the atmosphere (i.e., Coulomb scattering or drift into the loss cone), and charge exchange with the neutral hydrogen geocorona.

The model was used to simulate the hot ion distribution in near-Earth space for eight magnetic storm events. Table 1 lists the dates of these storms along with the UT of the storm sudden commencement (SSC), the UT of the Dst minimum, the value of the Dst minimum, the UT of the Dst* minimum (Dst* is Dst after removing magnetopause current effects and the diamagnetic influence of the Earth), and the value of the Dst* minimum. While all eight storms are driven by interplanetary coronal mass ejections, they have disparate solar wind and IMF time series, and they are from disparate solar cycle and seasonal phases.

Many quantities can be derived from the five-dimensional phase space density results from a simulation. One such quantity is the total energy content of the hot ions in the inner magnetosphere. The Dessler-Parker-Sckopke relation [*Dessler and Parker*, 1959; *Sckopke*, 1966] equates this value with the magnetic perturbation at the center of Earth resulting from the azimuthal current that these hot ions produce. The result is true regardless of local time symmetry in the ion distribution, but field-aligned and ionospheric closure currents for any asymmetries are not included in the result. This perturbation value can be directly compared

Table 1. Storm Characteristics

Storm	SSC UT	Dstmin UT	Dstmin	Dst*min UT	Dst* min
June 1991	16 UT, 6/4	19 UT, 6/5	-223	19 UT, 6/5	-232.1
May 1997	02 UT, 5/15	12 UT, 5/15	-115	11 UT, 5/15	-119.8
September 1998	00 UT, 9/25	09 UT, 9/25	-207	07 UT, 9/25	-199.6
October 1998	20 UT, 10/18	15 UT, 10/19	-112	04 UT, 10/19	-126
October 1999	16 UT, 10/21	06 UT, 10/22	-231	07 UT, 10/22	-247.1
April 2000	16 UT, 4/6	00 UT, 4/7	-321	00 UT, 4/7	-315.1
May 2000	17 UT, 5/23	08 UT, 5/24	-147	04 UT, 5/24	-169.1
July 2000	19 UT, 7/15	22 UT, 7/15	-300	22 UT, 7/15	-261.1

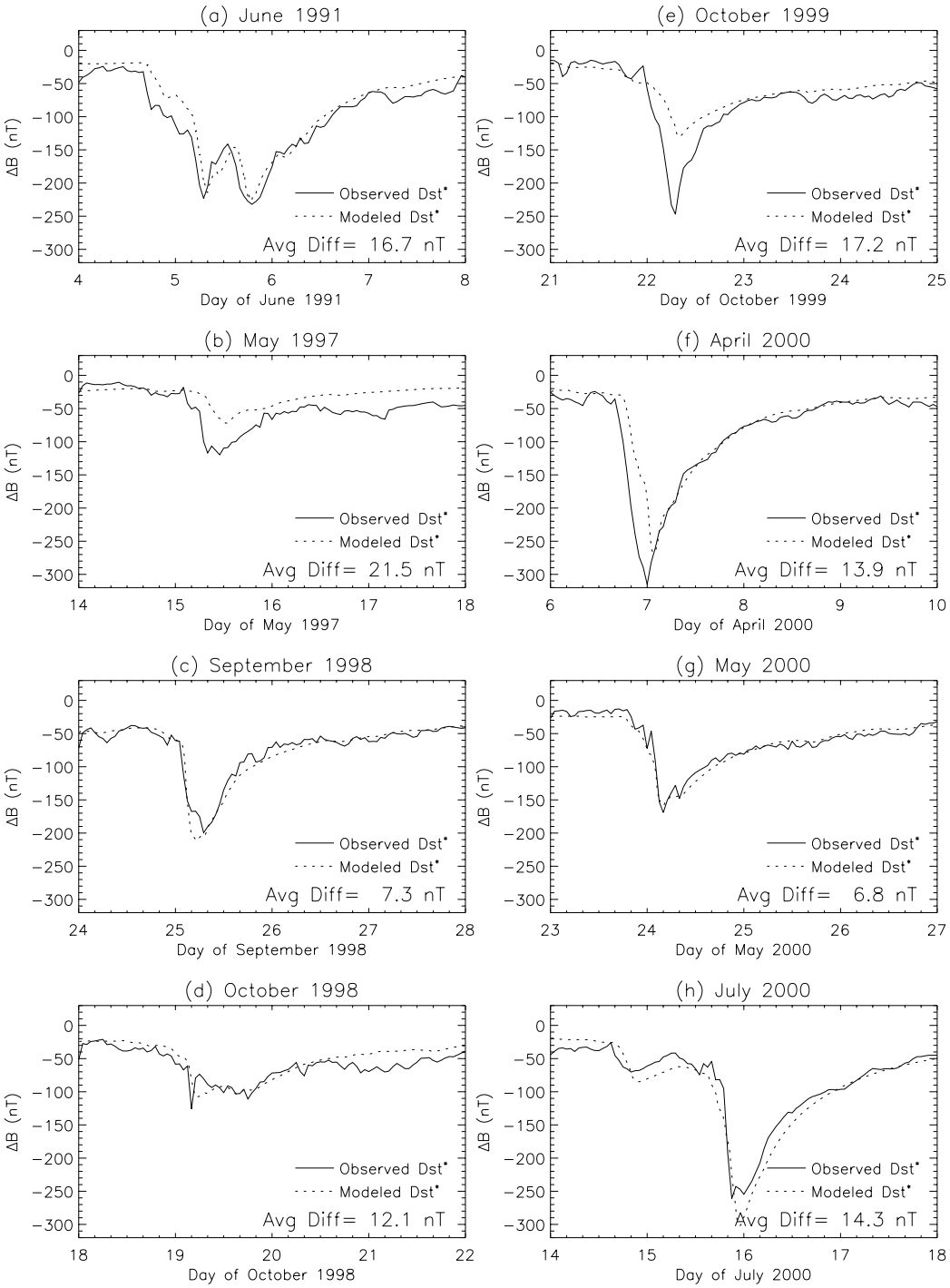

Figure 1. Observed and modeled Dst* for the eight storms considered in this study. Listed in each panel is the average of the absolute value of the difference between these two quantities.

against the observed Dst* to understand how well the model resproduces the stormtime ring current, and also how much of the observed Dst* is caused by the azimuthal currents from the ions in the simulation domain. A comparison of the observed and modeled Dst* values are shown in Figure 1. It is seen that the agreement is quite good for most of the storms, indicating that most of the observed Dst* perturbation is from the stormtime ring current (partial and asymmetric, i.e., everything in-

cluded in the simulation domain). Note that during the main phase and early part oft he recovery phase, for each storm, most of the modeled Dst* perturbation is from the asymmetric component of the ring current [e.g., *Liemohn et al.*, 2001a, b]. Listed in each panel is the average of the absolute value of the difference between the observed and modeled Dst* values. these values range from 6.8 nT to 21.5 nT. The trend is for the modeled values to be smaller in magnitude (that is, closer to zero) than the observed values, indicating that other current systems, summed together, contribute -10 to -20 nT to this index. Another feature of Figure 1 is that the overall shape of the time series of Dst* is similar between the observed and modeled Dst* values. This comparison lends support to the claim that the model is accurately calculating the storm-time ring current strength.

It was discussed in the previous section that substorms have little affect on the ion distribution below about 40 keV. Therefore, from the results of this model, it is possible to examine the relative contribution to the total energy content of the ring current from particles with magnetic moments in the MPA energy range with those in the SOPA energy range. This energy (40 keV at 6.6 R_E, defined hereinafter as an $E_{6.6}$ energy) can be adiabatically mapped throughout the simulation domain to determine the regions of phase space density above and below this $E_{6.6}$ value. This was done for all of the storm simulations. Figure 2 shows the result for the May 2000 storm. It is seen that at the peak of the storm (defined as the time of maximum energy content in the ring current), the ions with $E_{6.6}$<40 keV account for most of the total energy content. Before the storm, the contributions from the two $E_{6.6}$ ranges are roughly equal, but it is the lower-energy plasma sheet ions that enter most rapidly into the near-Earth region (comparing the line slopes just after the SSC). While the $E_{6.6}$>40 keV ions increase their inner magnetospheric content by a factor of two, the lower-energy ions increase their inner magnetospheric content by a factor of ten. The loss rates are different between the two $E_{6.6}$ ranges, however, with the lower-energy particles being preferrentially removed after the storm peak. By the end of the simulation, which is nearly three days after the storm peak, the $E_{6.6}$<40 keV range still dominates the total energy content.

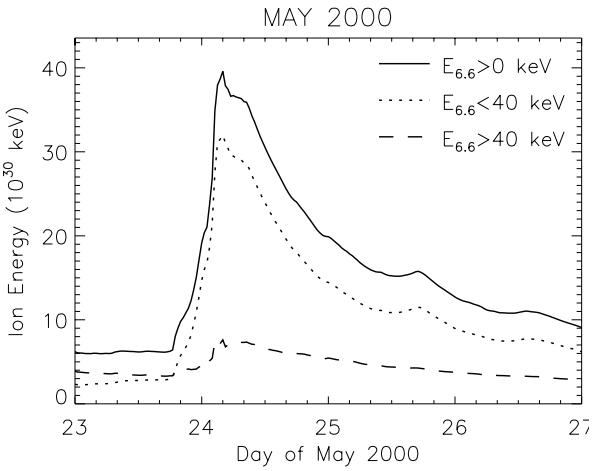

Figure 2. Total ion energy in the simulation during the May 2000 storm for the entire energy range (solid line), energies that map to $E_{6.6}$<40 keV (dotted line), and energies that map to $E_{6.6}$>40

Figure 3 shows the relative contribution from each energy range as a percent of the total ion energy content. Two curves are shown in the plot. The solid line gives the percent contribution from the $E_{6.6}$<40 keV range to the total ion content for that given time. However, to isolate the influence of access during the storm, the energy contents for each range at the SSC can be subtracted from the rest of the curves in Figure 2. Resulting negative values are set to zero for that $E_{6.6}$ range. The $E_{6.6}$<40 keV range percent contribution to the total energy, with this baseline adjustment, is given by the dotted line in Figure 3. It is seen that the solid curve in Figure 3 begins below 40% and slowly rises to ~45% by the SSC. It then increases to maximum value of 82% near the storm peak before slowly declining throughout the recovery phase, still up near 70% almost three days later. It shows that the lower-energy ions have a rapid response to the strong convection during the main phase, but are preferentially removed (albeit only slightly) during the recovery. The adjusted baseline curve in Figure 3 begins at 0% because the energy content of the $E_{6.6}$<40 keV ions is slowly increasing before the storm. After the SSC, the percentage jumps, reaching a maximum value of 93% before declining down to 84% a day or so later. The sharp rise followed the small dip indicates the preferential inflow and removal of the lower-energy ions during the storm. The curve then in-

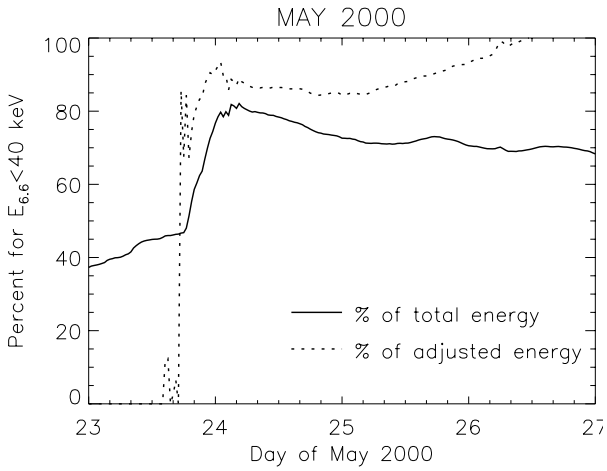

Figure 3. Percent of particle energy during the May 2000 storm carried by ions with energies that map to $E_{6.6}$<40 keV, as a function of total ion energy (dotted line) and as a function of total ion energy minus a prestorm baseline value (dotted line).

creases up to 100% as the $E_{6.6}$>40 keV ion energy content drops below its prestorm value.

The May 2000 storm is illustrative of the trend for all of the storms. Figures 4 and 5 give similar results as those shown in Figures 2 and 3, respectively, but for a superposed epoch analysis of all eight storm events. The fiducial for the superposition is the storm peak. In Figure 5, the baseline subtraction fiducial is defined as the SSC time for each storm, individually. In Figure 4, it is seen that the $E_{6.6}$<40 keV ions account for most of the energy content during the main and recovery phases. The $E_{6.6}$>40 keV ions show only a little growth during the storm sequence. This is most likely because of the sporadic timing of the rise of energy content for these ions. That is, the high-energy boundary condition flux increases with each substorm, but these occur randomly for each storm, and thus a systematic change in energy content for this range is not clearly evident. Figure 5 highlights this effect, with the $E_{6.6}$<40 keV ions containing 90% of the total ion energy at the storm peak, and >95% of the adjusted energy content (total minus a prestorm baseline) during the storm.

Note that these simulation results are in good agreement with those of *Wolf et al*. [1997] and *Fok et al*. [1999], who both found that substorm dipolarizations alone are insufficient to produce the stormtime ring current. From their idealized case studies, they showed that strong convection is the primary driver of plasma sheet particles into the near-Earth region. The present study goes a step farther, showing that it is the E<40 keV energy range from the plasma sheet that supplies most the stormtime ring current energy content, and that this energy range is relatively unaffected by substorms.

5. Discussion

Data show that substorms mainly influence the high-energy tail of the near-Earth plasma sheet ion distribution. There is not much (if any) systematic influence on ion in the E<40 keV range. Simulations, which accurately reproduce the observed Dst* values (within a reasonable error), show that the stormtime ring current is largely comprised of ions mapping to the E<40 keV energy range in the plasma sheet. These two results can be combined to conclude that substorms are not major contributors to the stormtime ring current, at least not directly.

That said, substorms are certainly an essential part of magnetic storms, and they contribute to the formation of the stormtime ring current through a number of indirect processes. During the growth phase, the thin current sheet preferentially accelerates heavy ions in the magnetotail [*Nosé et al*.,

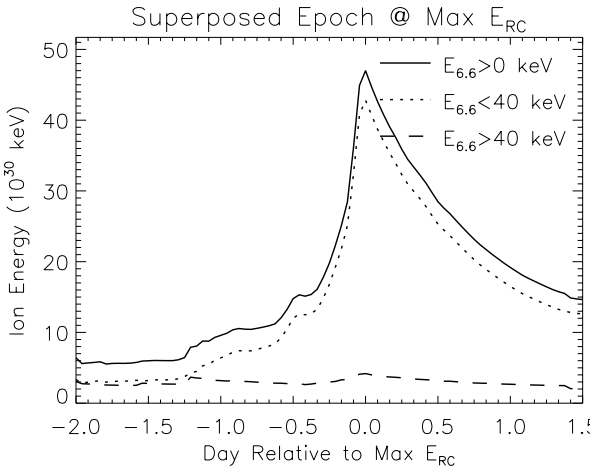

Figure 4. Total ion energy in the simulation as a superposed epoch of the 8 storms (time relative to the simulated maximum total ion energy) for the entire energy range (solid line), energies that map to $E_{6.6}$<40 keV (dotted line), and energies that map to $E_{6.6}$>40 keV (dashed line).

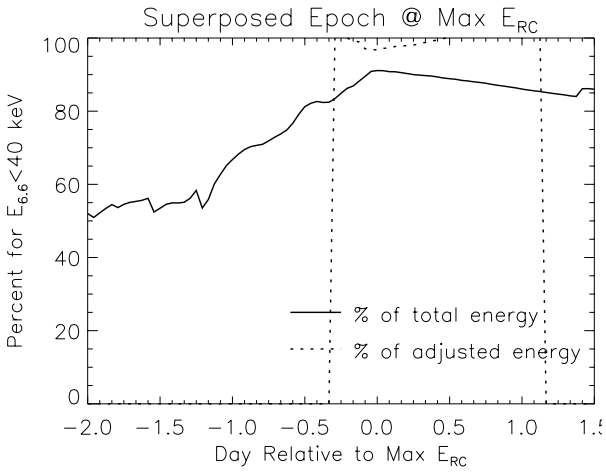

Figure 5. Percent of particle energy as a superposed epoch of the 8 storms (time relative to the simulated maximum total ion energy) carried by ions with energies that map to $E_{6.6}$<40 keV as a function of total ion energy (solid line) and as a function of total ion energy minus a prestorm baseline value (dotted line).

2001]. Substorms also alter the plasma sheet from the reconnection line to the inner edge of the dipolarization region, churning up and isotropizing the existing plasma distribution [e.g., *Onsager et al*., 1991]. Substorms also have a "directly driven" component, which is essentially enhanced convection, and is most likely inseparable from the large-scale convection driving the plasma sheet. Ionospheric outflow is also greatly enhanced during the expansion and growth phases of substorms [e.g., *Delcourt et al*., 1990; *Daglis and Axford*, 1996], pumping heavy ions into the tail for subsequent transport into the inner magnetosphere.

Note that there are caveats to the approach chosen for this study, most notably that the model is predisposed for convection dominance. It assumes a dipole magnetic field, which means there are no stretched B-field or dB/dt effects inside of the simulation domain. This also means that there are no inductive electric fields included (that is, all of the dipolarization occurs beyond geosynchronous orbit). However, substorms are indirectly included through boundary condition flux changes and variations in the cross polar cap potential. Finally, radial diffusion is only included through fluctuations of the cross polar cap potential (which has a 5-minute cadence in these simulations). While these fluctuations cause a small amount of radial diffusion, it is not to the level of that included in the *Chen et al*. [1993] study, which showed that this process is significant for the high-energy range during storms with long main phases (> 6 hours).

6. Conclusion

Using simulation results of the stormtime ring curent, it has been shown that substorms, which mainly influence the high-energy tail of the ion distribution in the near-Earth plasma sheet, do not directly contribute in any significant amount to the creation of the ring current. This result is very similar to the findings of *Wolf et al*. [1997] and *Fok et al*. [1999], except that instead of examining results from idealized simulation studies, the present investigation has used simulation results for eigth real storms over the past solar cycle. While additional work is needed to compare in situ and remote sensing observations of the stormtime ring current against these simulation results, previous data-theory comparisons with this model and the agreement with the observed Dst* values for the chosen storms lends support to the validity of these results.

Acknowledgments
This study was supported by grants from the NASA Geospace Sciences and Living With a Star programs and the NSF Magnetospheric Physics program.

References

Akasofu, S.-I., and S. Chapman, The ring current, geomagnetic disturbance and the Van Allen radiation belts, *J. Geophys. Res.*, **66**, 1321, 1961.

Birn, J., M. F. Thomsen, J. E. Borovsky, G. D. Reeves, D. J. McComas and R. D. Belian, Characteristic plasma properties during dispersionless substorm injections at geosynchronous orbit, *J. Geophys. Res.*, **102**, 2309, 1997a.

Birn, J., M. F. Thomsen, J. E. Borovsky, G. D. Reeves, D. J. McComas, R. D. Belian, and M. Hesse, Substorm ion injections: Geosynchronous observations and test particle orbits in three-dimensional dynamic MHD fields, *J. Geophys. Res.*, **102**, 2325, 1997b.

Burton, R. K., R. L. McPherron, and C. T. Russell, An empirical relationship between interplanetary conditions and Dst, *J. Geophys. Res.*, **80**, 4204, 1975.

Chen, M. W., M. Schulz, L. R. Lyons, and D. J. Gorney, Stormtime transport of ring current and radiation belt ions, *J. Geophys. Res.,* **98**, 3835, 1993.

Daglis, I. A., and W. I. Axford, Fast ionospheric response to enhanced activity in geospace: Ion feeding of the inner magnetotail, *J. Geophys. Res.*, **101**, 5047, 1996.

Delcourt, D. C., J. a. Sauvaud, and A. Pedersen, Dynamics of single-particle orbits during substorm expansion phase, *J. Geophys. Res.*, **95**, 20,853, 1990.

Dessler, A. J., and E. N. Parker, Hydromagnetic theory of geomagnetic storms, *J. Geophys. Res.,* **64**, 2239, 1959.

Fok, M.-C., J. U. Kozyra, A. F. Nagy, C. E. Rasmussen, and G. V. Khazanov, Decay of equatorial ring current ions and associated aeronomical consequences, *J. Geophys. Res.,* **98**, 19,381, 1993.

Fok, M.-C., T. E. Moore and D. C. Delcourt, Modeling of inner plasma sheet and ring current during substorms, *J. Geophys. Res*., **104**, 14557, 1999.

Ganushkina, N. Yu., et al., Entry of plasma sheet particles into the inner magnetosphere as observed by Polar/CAMMICE, *J. Geophys. Res.*, **105**, 25,205, 2000.

Ganushkina, N. Yu., T. I. Pulkkinen, V. F. Bashkirov, D. N. Baker, and X. Li, Formation of intense nose structures, *Geophys. Res. Lett.*, **28**, 491, 2001.

Gonzalez, W. D., J. A. Joselyn, Y. Kamide, H. W. Kroehl, G. Rostoker, B. T. Tsurutani, and v. M. Vasyliunas, What is a geomagnetic storm?, *J. Geophys. Res.,* **99**, 5771, 1994.

Grande, M., C. H. Perry, A. Hall, J. Fennell, and B. Wilken, Statistics of substorm occurrence in storm and non-storm periods, *Phys. Chem. Earth,* **24**, 167, 1999.

Jordanova, V. K., L. M. Kistler, J. U. Kozyra, G. V. Khazanov, and A. F. Nagy, Collisional losses of ring current ions, *J. Geophys. Res.,* **101**, 111, 1996.

Li, X., I. Roth, M. Temerin, J. R. wygant, M. K. Hudson, and J. B. Blake, Simulation of the prompt energization oand transport of radiation belt particles during the March 24, 1991 SSC, *Geophys. Res. Lett.*, **20**, 2433, 1993.

Li, X., D. N. Baker, M. Temerin, G. D. Reeves, and R. D. Belian, Simulation of dispersionless injections and drift echoes of energetic electrons associated with substorms, *Geophys. Res. Lett.*, **25**, 3763, 1998.

Liemohn, M. W., J. U. Kozyra, M. F. Thomsen, J. L. Roeder, G. Lu, J. E. Borovsky, and T. E. Cayton, Dominant role of the asymmetric ring current in producing the stormtime Dst*, *J. Geophys. Res.,* **106**, 10,883, 2001a.

Liemohn, M. W., J. U. Kozyra, C. R. Clauer, and A. J. Ridley, Computational analysis of the near-Earth magnetospheric current system, *J. Geophys. Res.,* **106**, 29,531, 2001b.

McIlwain, C. E., A Kp dependent equatorial electric field model, *Adv. Space Res.,* **6**(3), 187, 1986.

Nosé, M., S. Ohtani, K. Takahashi, A. T. Y. Lui, R. W. McEntire, D. J. Williams, S. P. Christon, and K. Yumoto, Ion composition of the near-Earth plasma sheet in storm and quiet intervals: Geotail/EPIC measurements, *J. Geophys. Res.,* **106**, 8391, 2001.

Onsager, T. G., M. F. Thomsen, R. C. Elphic, and J. T. gosling, Model of electron and ion distributions in the plasma sheet boundary layer, *J. Geophys. Res.,* **96**, 20,999, 1991.

Sarris, T. E., X. Li, N. Tsaggas, and N. Paschalidis, Modeling energetic particle injections in dynamic pulse fields with varying propagation speeds, *J. Geophys. Res.*, **107**, 10.1029/2001JA900166, 2002.

Sckopke, N., A general relation between the energy of trapped particles and the disturbance field near the Earth, *J. Geophys. Res.,* **71**, 3125, 1966.

Sheldon, R.B., and D. C. Hamilton, Ion transport and loss in the Earth's quiet ring current. 1. Data and standard model, *J. Geophys. Res*., **98**, 13,491, 1993.

Thomsen, M. F., J. E. Borovsky, D. J. McComas, and M. R. Collier, Variability of the ring current source population, *Geophys. Res. Lett,* **25**, 3481, 1998.

Tsurutani, B. T., and W. D. Gonzalez, The cause of high intensity long-duration continuous AE activity (HILDCAAs): Interplanetary Alfvén wave trains, *Planet. Space Sci.,* **35**, 405, 1987.

Wolf, R. A., J. W. freeman, Jr., B. A. Hausman, R. W. Spiro, R. V. Hiilmer, and R. L. Lambour, Modeling convection effects in magnetic storms, in *Magnetic Storms, Geophys. Monogr. Ser.*, **98**, edited by B. T. Tsurutani, W. D. Gonzalez, Y. Kamide, and J. K. Arballo, American Geophysical Union, 161, 1997.